Applied Mathematical Sciences, Vol. 1, 2007, no. 44, 2187 - 2201

Choice of Rererence Images for Video Compression

Mohammed Benabdellah, Fakhita Regragui, Mourad Gharbi and El Houssine Bouyakhf

Université Mohamed V - Agdal
LIMIARF - Faculté des sciences
4 Avenue Ibn Battouta
B.P. 1014 RP, Rabat - Maroc

Abstract

In this work, we experiment with the choice of reference images, in the process of video compression, by using only the intra and predicted images extracted from sequences. For intra and predicted image, we apply the Faber-schauder Multi-scale Transform (FMT). Then, each image is compared with the other images by subtracting corresponding images transformed by FMT. The choice of the best reference image is based on the result of subtraction. We adopt the criterion of minimum pixels if the resulting images present only points and the criterion of minimum distance between the curves if they present parallel linear or nonlinear curves, and possibly points. Testing this approach on video sequences revealed an improvement in data flow and average PSNR as compared to the original encoding and choosing reference images based on the mean square error.

Keywords: Image processing, MSE, PSNR, Multi-scale base of Faber-Schauder, MPEG, H.26x.

1 Introduction

During the last few years, interest in multimedia and in particular diffusion of the audio-visual content involved a great amount of research in the field of video signal coding, which led to several standards such as H-263, H.26L and MPEG-4 [14]. These standards consist essentially of toolboxes for video signal processing which can be adapted to the context and desired result (flow/distortion report)[8]. Recent research aims to improve these tools and set froth new ones. In this paper, we first introduce the techniques used in the

video compression process. Then, we present the Faber-Schauder Multi-scales Transformation (FMT), which carries out a change of the canonical base towards that of Faber-Schauder. We use an algorithm of transformation (and reverse transformation), which is fast and exact. Next, we present a method of visualization at mixed scales which makes it possible to observe, on only one image, the effect of the transformation. We notice a concentration of coefficients around the outline areas. Lastly, we will explain the stages followed in our experiments and the results found, after the application and comparison with the original sequence and the method that uses MSE to find the best reference images.

2 Methods

2.1 Structure of coding

The techniques used to compress a video signal use space redundancy. The objective is to reduce the flow of the video sequence to be compressed, while minimizing the visible errors (MSE and PSNR)[3]. To do this, there are two principal techniques, lossless compression and lossy compression [22]. The former makes it possible to find the initial information after decompression, while the latter will restore only an approximation of it [16]. In the case of natural images, the lossless compression is insufficient, and the introduction of losses in the compression process makes it possible to obtain better results without preventing the interpretation of the visual content [7]. Current video standards use a hybrid coding system with compensation for movement based on blocks and a reduction of entropy by a transformer [8]. The MPEG standard defines a set of coding stages that transform a video signal (digitized in standardized format) into a binary stream (a bit stream) intended to be stored or transmitted through a network. The binary stream is described according to a syntax coded in a standardized way that can be restored easily by any decoder that recognizes the MPEG standard [9]. The coding algorithm defines a hierarchical structure containing the levels described in the following figure [2]:

The group of pictures or GOP consists of a periodic continuation of compressed images. There are three types of the compressed images [1]: an image of type I (Intra) compressed using JPEG for the fixed images. An image of type P (Predicted) coded using a prediction of a previous image of type I or P. An image of the type B (Bidirectional) coded by double prediction (or Interpolation) by using a previous image of type I or P and a future image of type I or P as references [16]. A GOP starts with an image I, contains a periodic continuation of the images P separated by a constant number of images B as in the following figure [6]. The structure of GOP is thus defined by two

Sequence	Heading	GOP	.....	GOP
GOP	Heading	Image	.....	Image
Image	Heading	Slice	.....	Slice
Slice	Heading	Macro-Block	.....	Macro-Block
Macro-Block	Heading	Block	.....	Block
Block	Heading	Coefficiemt	.....	Coefficient

Figure 1: Hierarchical structure of MPEG coding.

parameters: the number of images of GOP and the distance between images I and P [5].

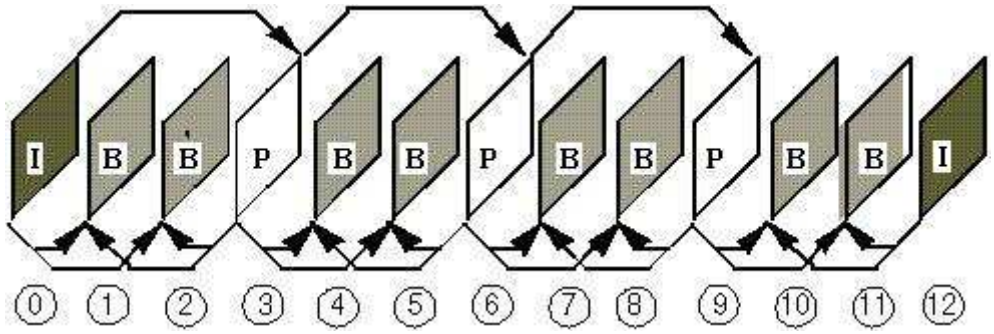

Figure 2: Structure of GOP.

2.2 Construction of the Faber-Schauder multiscale base

The Faber-Schauder wavelet transform is a simple multiscale transformation with many interesting properties in image processing. In these properties, we advertise multiscale edge detection, preservation of pixels ranges, elimination of the constant and the linear correlation...
For the construction of the Faber-Schauder base, we suppose the family of under spaces $(W_j)_{j\in Z}$ of $L^2(R^2)$ such as V_j is the direct sum of V_{j+1} and W_{j+1} [9]:

$$\begin{cases} V_j = V_{j+1} \oplus W_{j+1} \\ W_{j+1} = (V_{j+1} \times W_{j+1} \oplus W_{j+1} \times V_{j+1} \oplus W_{j+1} \times W_{j+1}) \end{cases}$$

The space base W_{j+1} is given by:
$(\psi^{j+1}_{1,k,l} = \phi^j_{2k+1} \times \psi^{j+1}_l, \psi^j_{2,k,l} = \psi^{j+1}_k \times \phi^j_{2l}, \psi^j_{3,k,l} = \psi^{j+1}_k \times \psi^{j+1}_l)_{k,l\in Z}$
and the unconditional base and Faber-Schauder multi-scale of $L^2(R^2)$ is given by: $(\psi^m_{1,k,l}, \psi^m_{2,k,l}, \psi^m_{3,k,l})_{k,l,m\in Z}$

A function of V_0 : $f(x,y) = \sum_{k,l\in Z} f^0_{k,l}\phi^0_{k,l}(x,y)$ can be broken up in a single way according to V_1 and W_1 [12]:
$f(x,y) = \sum_{k,l\in Z} f^1_{k,l}\phi^1_{k,l}(x,y) + \sum_{k,l\in Z}[g^{11}_{k,l}\psi^1_{k,l}(x,y) + g^{21}_{k,l}\psi^2_{k,l}(x,y) + g^{31}_{k,l}\psi^3_{k,l}(x,y)]$.
The continuation f^1 is a coarse version of the original image f^0(a polygonal approximation of f^0), while $g^1 = (g^{11}, g^{21}, g^{31})$ represents the difference in information between f^0 and f^1 . g^{11}(respectively g^{21}) represents the difference for the first (respectively the second) variable and g^{31} the diagonal represents difference for the two variables [11].
The continuations f^1 and g^1 can be calculated starting from f^0 in the following way:

$$\begin{cases} f^1_{k,l} = f^0_{2k,2l} \\ g^{11}_{k,l} = f^0_{2k+1,2l} - 1/2(f^0_{2k,2l} + f^0_{2k+2,2l}) \\ g^{21}_{k,l} = f^0_{2k,2l+1} - 1/2(f^0_{2k,2l} + f^0_{2k,2l+2}) \\ g^{31}_{k,l} = f^0_{2k+1,2l+1} - 1/4(f^0_{2k,2l} + f^0_{2k,2l+2} + f^0_{2k+2,2l} + f^0_{2k+2,2l+2}) \end{cases}$$

Reciprocally one can rebuild the continuation f^0 from f^1 and g^1 by :

$$\begin{cases} f^0_{2k,2l} = f^1_{k,l} \\ f^0_{2k+1,2l} = g^{11}_{k,l} + 1/2(f^1_{k,l} + f^1_{k+1,l}) \\ f^0_{2k,2l+1} = g^{11}_{k,l} + 1/2(f^1_{k,l} + f^1_{k,l+1}) \\ f^0_{2k+1,2l+1} = g^{31}_{k,l} + 1/4(f^1_{k,l} + f^0_{k,l+1} + f^1_{k+1,l} + f^1_{k+1,l+1}) \end{cases}$$

We thus obtain a pyramidal algorithm which, on each scale j, decompose (respectively reconstructed) the continuation f^j in (respectively from) f^{j+1} and g^{j+1} [23]. The number of operations used in the algorithm is proportional to the number N of data, which is not invalid in the signal ($O(N)$) what makes of it a very fast algorithm [24]. What is more, the operations contain only arithmetic numbers; therefore, the transformation is exact and does not produce any approximation in its numerical implementation [14].
The FMT Transformation has exactly the same principle of construction as that of Mallat except that the canonical base of the multi-resolution analysis is not an orthogonal base [25]. This does not prevent it from having the same properties in image processing as the wavelets bases [7]. In addition, the FMT algorithm is closer to that of the laplacian pyramid, because it is very simple and completely discrete, what makes it possible to observe directly on the pixels the effects of the transformation. In short, the FMT transformation is a good compromise between the wavelets bases and the diagram of the laplacian pyramid [14].

2.3 Visualization of the transformed images by the FMT

The result of the wavelets transformation of an image is represented by a pyramidal sequence of images, which includes the differences in information between the successive scales (figure3) [5].

However, we can consider the FMT multi-scale transformation as a linear

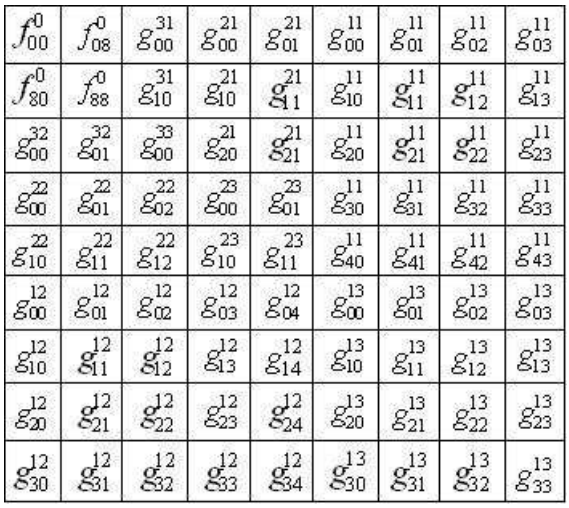

Figure 3: Representation on separated scales for 9×9 transformed image in the multi-scale base

application, from the canonical base to the multi-scale base, which distributes the information contained in the initial image in a different way. It is thus more natural to visualize this redistribution, in the multi-scale base, in only one image, as it is the case in the canonical base. The principle of the visualization of images in the canonical base consists in placing each coefficient at the place where its basic function reaches its maximum. The same principle is naturally essential for the multi-scale base (Figure 4) [14].
The image obtained is a coherent one which resembles an outline representation of the original image (Figure 5). Indeed, the FMT transformation, like some wavelets transformation, has similarities with the canny outlines detector [19], where the outlines correspond to the local maximum in the module of transformation. In fact, in the case of the FMT transformation, on each scale, the value of each pixel is given by the calculation of the difference with its neighboring of the preceding scale. Thus the areas which present a local peak for these differences correspond to a strong luminous transition for the values of grey, while the areas, where those differences are invalid, are associated with an area, where the level of grey is constant [18].

f_{00}^{0}	g_{00}^{11}	g_{00}^{21}	g_{01}^{11}	g_{00}^{31}	g_{02}^{11}	g_{01}^{21}	g_{03}^{11}	f_{08}^{0}
g_{00}^{12}	g_{00}^{13}	g_{01}^{12}	g_{01}^{13}	g_{02}^{12}	g_{02}^{13}	g_{03}^{12}	g_{03}^{13}	g_{04}^{12}
g_{00}^{22}	g_{10}^{11}	g_{00}^{23}	g_{11}^{11}	g_{01}^{22}	g_{12}^{11}	g_{01}^{23}	g_{13}^{11}	g_{02}^{22}
g_{10}^{12}	g_{10}^{13}	g_{11}^{12}	g_{11}^{13}	g_{12}^{12}	g_{12}^{13}	g_{13}^{12}	g_{13}^{13}	g_{14}^{12}
g_{00}^{32}	g_{20}^{11}	g_{10}^{21}	g_{21}^{11}	g_{00}^{33}	g_{22}^{11}	g_{11}^{21}	g_{23}^{11}	g_{01}^{32}
g_{20}^{12}	g_{20}^{13}	g_{21}^{12}	g_{21}^{13}	g_{22}^{12}	g_{22}^{13}	g_{23}^{12}	g_{23}^{13}	g_{24}^{12}
g_{10}^{22}	g_{30}^{11}	g_{10}^{23}	g_{31}^{11}	g_{11}^{22}	g_{32}^{11}	g_{11}^{23}	g_{33}^{11}	g_{12}^{22}
g_{30}^{12}	g_{30}^{13}	g_{31}^{12}	g_{31}^{13}	g_{32}^{12}	g_{32}^{13}	g_{33}^{12}	g_{33}^{13}	g_{34}^{12}
f_{80}^{0}	g_{40}^{11}	g_{20}^{21}	g_{41}^{11}	g_{10}^{31}	g_{42}^{11}	g_{21}^{21}	g_{43}^{11}	f_{88}^{0}

Figure 4: Representation on mixed scales, the coefficients are placed at the place where their basic functions are maximal

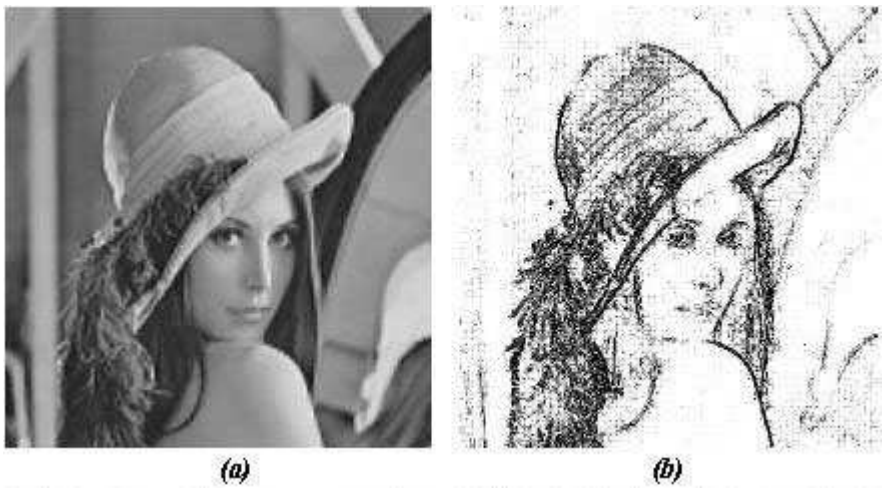

Figure 5: Representation on mixed-scales and on separate scales of the image "Lena". The coefficients are in the canonical base in (a) and in the Faber-Schauder multi-scale base in (b)

2.4 Compression of images by FMT

A worthwhile priority over the FMT transformation, which is also valid for the wavelets transformations, is the characteristic aspect observed in the histograms of transformed images: the number of coefficients for a given level of grey decreases very quickly, to practically fade away, when we move away

from any central value very close to zero (Figure 6) [11]. This implies that the information (or the energy) of the transformed image is concentrated in a small number of significant coefficients, confined in the outline region of the initial image [10] . Therefore, the cancelation of other coefficients (almost faded away) only provokes a small disruption of the transformed image. In order to know the effect of such disruption in the reconstruction of the initial image one should calculate the matrix conditioning of the FMT transformation [12]. In fact, if we have f = Mg where f is the initial image and g is the multi-scale image, then the conditioning of M ($Cond(M) = ||M||.||M^{-1}|| \geq 1$) who checks: $||\delta f||/||f|| \leq Cond(M)||\delta g||/||g||$. This means that the relative variation of the restored image cannot be very important, with reference to the multi-scale image, if the conditioning is closer to 1 [13].

For the orthonormal transformations, the conditioning is always equal to 1; thus it is optimum. However, we can always improve the conditioning if we are able to multiply each column (or each line) by a well chosen scalar; in the case of a base changing, this pushes a change in the normalization of the base elements [4].

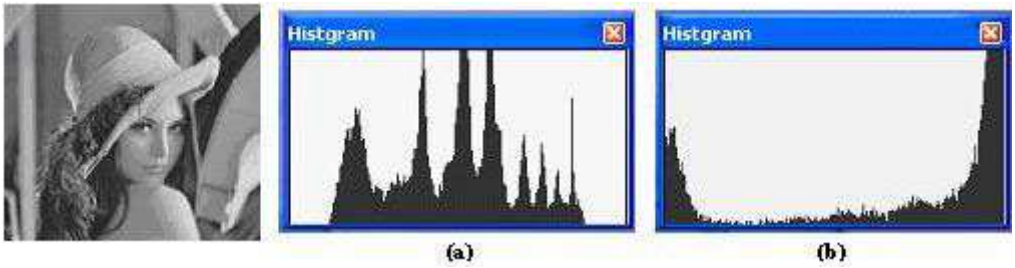

Figure 6: Histograms of image " Lena ": (a) in the canonical base, (b) in the multi-scale base

2.5 The paper Problems

Traditionally speaking, the reference image used during the encoding of a predicted image is not chosen. However, it is the previous image of the type P or I, which is used instead. However, in certain cases, the choice of an image located further in the sequence would seem more suitable [18].
As a first example, let's take the case of a change of a repetitive plan. If a change of a plan occurs between two predicted images, the prediction of the first image of the second plan will be made from an image of the previous plan, whereas it would seem more interesting to use a former image of the same plan (if such an image exists). This problem is perfectly illustrated on the News sequence of figure 7 where the predicted image 69 refers to an image

of the plan B, whereas images of plan A were already coded later on (see the predicted image 63) [19].

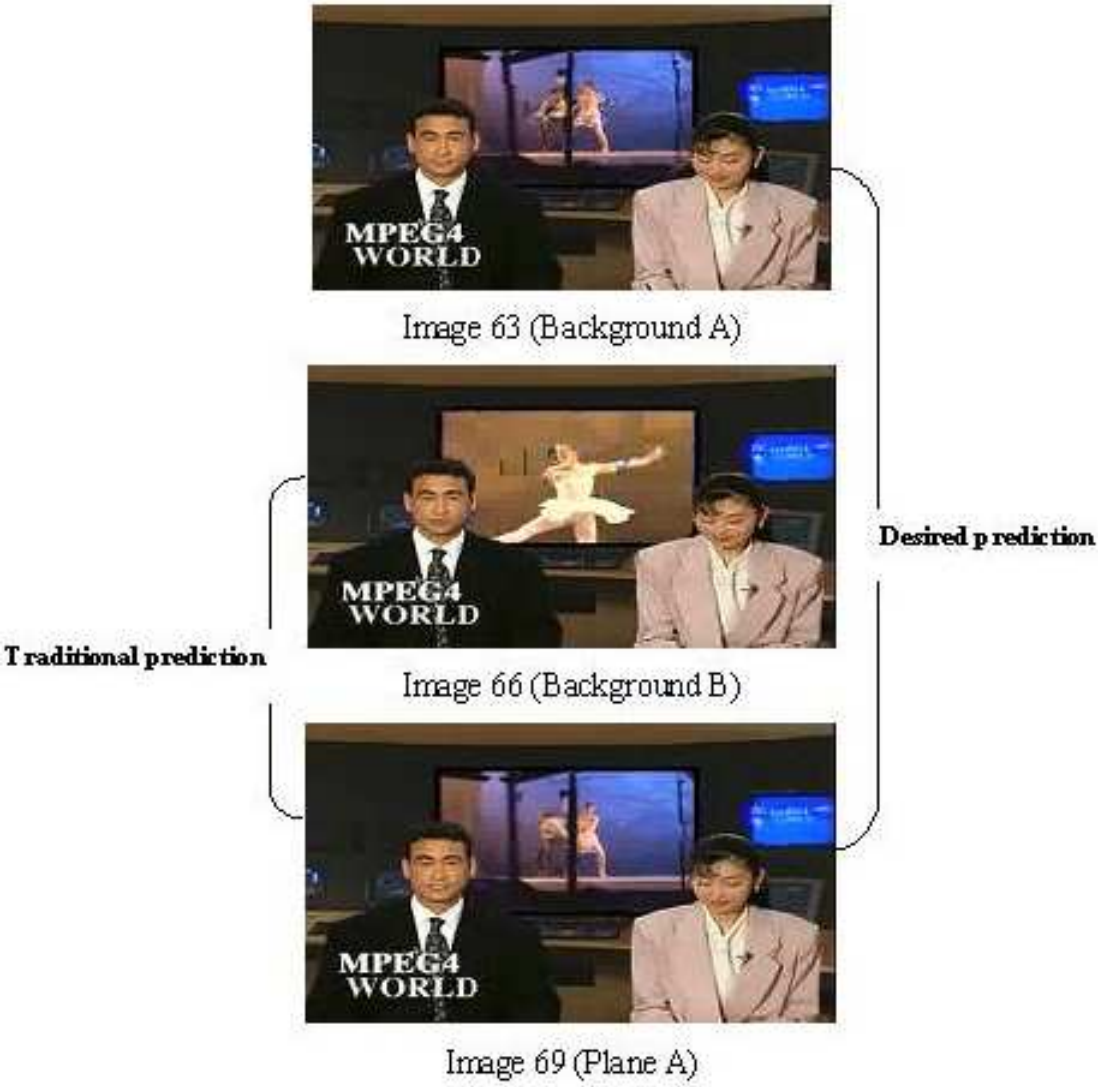

Figure 7: Prediction during a background change (News sequence)

The second example concerns the entry of an object in a scene as the images of the Kiss cool scene, which is consisted of 713 images, show below in figure 8. In this case, it would seem interesting to choose as a reference image the one where the object is completely returned in the field of vision. Therefore, the prediction would be more effective for the visible parts of the object for each image where it appears [20].

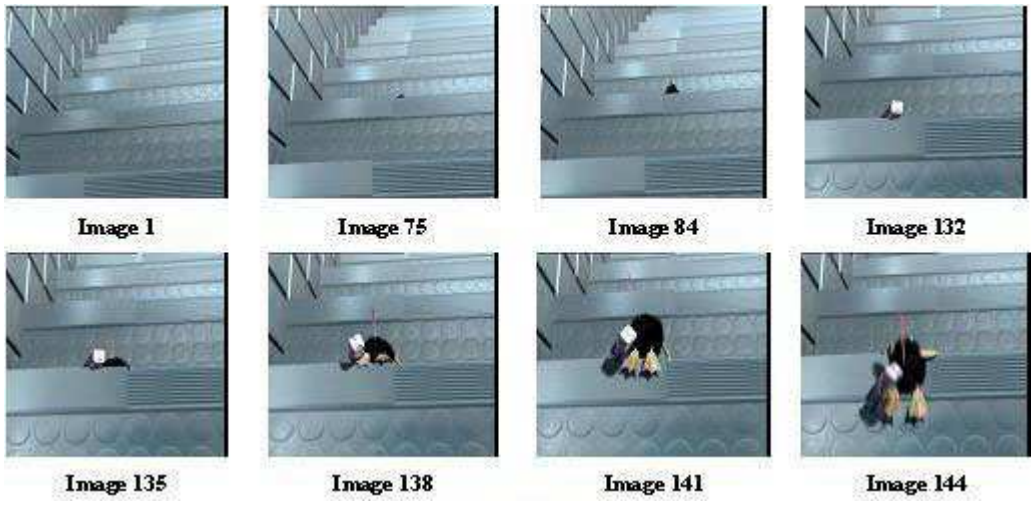

Figure 8: The kiss cool sequence

2.6 Diagram of the introduced method

The proposed method is introduced by the figure 9. The algorithm of the method suggested consists in extracting the various images initially; Intra image, Predicted image and Bidirectional image constituting the video sequence [14]. We apply the edges detection on Intra and Predicted images. Then, we make the subtraction between the edges images. We choose the best reference image for each image as follows:

- If we will have results, after subtraction of edges images, containing only the points, we choose the best reference image for the concerned image, that which corresponds to the result containing the minimum number of points.

- If we will have results containing the points and the parallel linear or nonlinear curves. We choose the best reference image for the concerned image that which corresponds to the result containing the minimal distance between parallel linear or nonlinear curves.

3 Results

3.1 Research of the best intra image

Admitting that the reconstruction of sequences permit to choose the Intra image of a GOP, we would like to observe the influence of the choice of the Intra

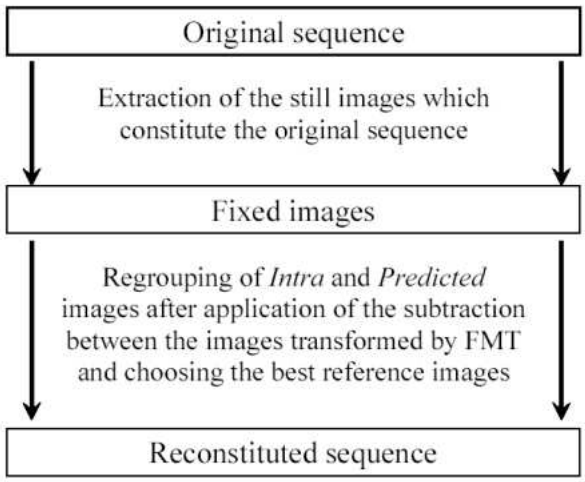

Figure 9: The proposed methodology

image on the quality of compression (in the flow/distorsion direction). People provided a script, which permits, for a given GOP, to test the encoding with each image of the GOP as an Intra image, and to provide a graph representing the storage costs of the images P and the PSNR average of the decoded images of each encoding [21]. The result of the execution of this script on the Kiss cool sequence for the GOP including the images from 78 to 90 can be seen in the figure 10. A gain is noticed at the level of the storage for the encoding of the sequence through using the second image (image 79) as an Intra image. Good results are not obtained in the following images. The use of the image 81 produces an equivalent result (a quite higher storage, but lower distortion). To obtain good results, we are going to reorder the sequence completely.

3.2 Regrouping of images and applications

The process consists of first gathering the similar images based on edge detection of Intra and Predicted images. Second, we perform a subtraction between the images in question and the other Intra and Predicted images of the GOP. The selected image of reference is the one whose edge subtraction with the image in question produces either the fewest points or maintains the same minimal distance between lines of points. A new sequence is then reconstructed image by image, through comparing each image with the others to select the nearest one. Later on, a search for the best Intra image is carried out for each GOP of the sequence. Once all of this information is gathered, the sequence to be encoded is then reconstructed. The results of this method on the sequence News (images 72-93) and on the sequence Kiss cool (images 144-165) are given

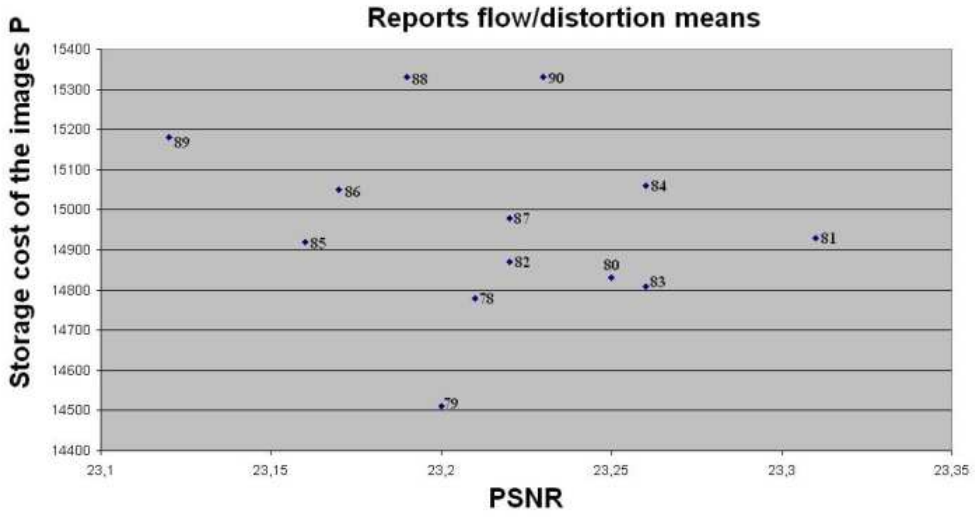

Figure 10: Flow/distortion report of the various Intra images of the GOP 78-90 in the Kiss Cool sequence

as follows:

News sequence:

After the regrouping of the News sequence, the image number 2 (the Predicted image number 2 of the GOP1) take the image number 0 (the Intra image of the GOP1) us reference image. Then, the image number 5 (the Predicted image number 1 of the GOP2) use the image number 2 (the Predicted image number 2 of the GOP1) us reference image. Next, the image number 6 (the Predicted image number 2 of the GOP2) use the image number 3 (the Predicted image number 3 of the GOP1) us reference image.

Kiss Cool sequence:

After regrouping of the Kiss cool sequence, the image number 3 (the Predicted image number 3 of the GOP1) take the image number 5 (the Predicted image number 1 of the GOP2) us reference image. Then, the image number 5 (the Predicted image number 1 of the GOP2) use the image number 6 (the Predicted image number 2 of the GOP2) us reference image. Next, the image number 6 (the Predicted image number 2 of the GOP2) use the image number 7 (the Predicted image number 3 of the GOP2) us reference image.

The regrouping of the sequence was efficient since the images were gathered by background. For same visual quality, the flow obtained with the regrouping of the sequence is much better than that obtained by original sequence and that obtained by the method which uses the MSE to deduce the similar images

	Original encoding of the sequence		Encoding by the method using MSE		Encoding by the introduced method	
	Flow (Kbit/s)	Average PSNR (dB)	Flow (Kbit/s)	Average PSNR (dB)	Flow (Kbit/s)	Average PSNR (dB)
The News sequence	1367.73	38.036927	1061.71	38.051430	1042.78	38.056525
The Kiss Cool sequence	1137.33	40.015128	832.67	40.032513	818.81	40.037601

Figure 11: The results, given in flow and average PSNR, obtained after the application of the original encoding, the encoding by the method uses the MSE and the introduced method

and to reconstruct the sequence of the images. We notice that this introduced method concerns the reduction of information for a minimal storage and a transmission by reduced flow. The visualization of the video sequences is carried out by call to the original regrouping of images.

4 Conclusion

The main idea behind this paper is to carry out tests on the modification of the encoding sequence of the video sequence images to produce a gain in the result. Some tests highlighted a possible gain for certain sequences through the choice of the reference images. Our method improves upon the MSE method in terms of being able to determine similar images and gather them before applying the encoding. We hope to apply this method to any type of image in the GOPs including bidirectional images. The FMT transformation is distinguished by its simplicity and its performances of seclusion of the information in the outline regions of the image. The mixed-scale visualization of the transformed images allows putting in evidence its properties, particularly, the possibilities of compression of the images and the improvement of the performances of the other standard methods of compression as JPEG and GIF.
ACKNOWLEDGEMENTS.

References

[1] Codage vidéo pour communication à faible débit, *UIT-T. Recommandation H.263*, version 2, 1998.

[2] Rob Koenen, Overview of the MPEG-4 standard,*iso/iecjtc1/sc29/wg 11 n4030*, Mars 2001.

[3] Joint Video Team (JVT) of ISO/IEC MPEG and ITU-T VCEG, Joint Final Commitee Draft (JFCD) of Joint Vidéo Specification (ITU-T Rec. H.264 - ISO/IEC 14496-10 AVC).

[4] Majid Rabbani, Paul W. Jones, Digital Image Compression Techniques, volume 7 of tutorial texts in optical engineering. *SPIE Optical Engineering Press*, Bellingham, WA, USA, 1991.

[5] Henri Nicolas, Contribution à la création et à la manipulation des objets vidéo, *PhD thesis*, Université de Rennes 1, Institut de Formation Supérieure en Informatique et Communication, 2001.

[6] M. Irani, P. Anandan, J. Bergen, R. Kumar et S. Hsu, Efficient representations of video sequences and their applications, *Signal Processing : Image Communication*, 8:327-351, 1996.

[7] Charles WAGNER , De l'image vers la compression, *Rapport de Recherche de l'INRIA*, Septembre 1993, France.

[8] Jacques GUICHARD, Dominique NASSE, Traitement des images Numériques pour la réduction du débit binaires, *CENT-Paris*, CCETT, France.

[9] Grégoire MERCIER, Christian ROUX, Gilbert MARTINEAN, Technologie du Multimédia, *ENST Bretagne, F-29280 Brest*, France, 15 Janvier 2003.

[10] H.Douzi, D.Mammass and F.Nouboud, Amélioration de la Compression des Images par la Transformation Multi-Echelle de Faber-Schauder, *Vision Interface'99*, Trois-Rivières, Canada, May 19-21, 1999.

[11] M. Benabdellah, M. Gharbi, N. Lamouri, F. Regragui, E. H. Bouyakhf, Adaptive compression of images based on Wavelets, *International Georgian Journal of Computer Sciences and Telecommunications*, No.1(8), pp.32-41, 31 March 2006.

[12] S.G.Mallat and S.Zhong, Characterization of Signals from Multiscale Edges, *IEEE Trans. On Pattern Analysis and Machine Intelligence*, Vol 14, No 7, July 1992.

[13] Laurent GARDES, Estimation d'une fonction quantile extreme, *Thèse de Doctorat de l'Université Montpellier II*, 06 Octobre 2003, France.

[14] M. Benabdellah, M. Gharbi, F. Regragui, E. H. Bouyakhf, A method for choosing reference images based on edge detection for video compression, *International Georgian Journal of Computer Science and Telecommunications*, No.3(7), pp.33-39, 25 December 2005.

[15] M. Benabdellah, M. Gharbi, N. Lamouri, F. Regragui, E. H. Bouyakhf, Adaptive compression of cartographic images based on Haar's wavelets, *International Moroccan Journal Physical and Chimical News*, 31 November 2005.

[16] M. Benabdellah, M. Gharbi, N. Lamouri, F. Regragui, E. H. Bouyakhf, A method for choosing reference images in video compression, *fifth IEEE-EURASIP International Symposium on COMMUNICATION SYSTEMS, NETWORKS AND DIGITAL SIGNAL PROCESSING (CSNDSP'06)*, Electrical and Computer Engineering Department, University of Patras, Patras, Greece,19-21 July, 2006.

[17] M. Benabdellah, M. Gharbi, F. Regragui, E. H. Bouyakhf, Adaptive compression based on wavelets of cartographic images, *IEEE International Computer Systems and Information Technology Conference (ICSIT'05)*, Algiers, July 19-21 2005.

[18] M. Benabdellah, M. Gharbi, F. Regragui, E. H. Bouyakhf, A method for choosing reference images based on edge detection for video compression, *4th International Multiconference on Computer Science and Information Technology (CSIT 2006)*. Applied Science Private University, Amman-Jordan, April 5-7 2006.

[19] M. Benabdellah, M. Gharbi, F. Regragui, E. H. Bouyakhf, Une méthode de choix des images de référence pour la compression des images animées, basée sur la détection des contours, *International Conference on Approximation Methods and Numerical Modeling in Environnement and Natural Resources (MAMERN'05)*, Oujda, Morocco May 09-11, 2005.

[20] M. Benabdellah, M. Gharbi, F. Regragui, E. H. Bouyakhf, Compression adaptative des images biomédicales basée sur les ondelettes, *Premières Journées Internationales de Mathématiques et Informatique d'oujda (JIMIO'1)*. Oujda, Maroc, 27-28 mai 2005.

[21] M. Benabdellah, M. Gharbi, F. Regragui, E. H. Bouyakhf, Adaptive compression of air images based on wavelets, *Rencontre Franco-Marocaine d'Approximation et d'Optimisation (RFMAO'2005)*, Rabat-Maroc, 19-20-21 Septembre 2005.

[22] M. Benabdellah, M. Gharbi, F. Regragui, E. H. Bouyakhf, Adaptive compression of cartographic images based on wavelets, *8èmes Journées d'Analyse Numérique et d'Optimisation (JANO8)*. ENIM-Rabat, 14-16 Décembre 2005.

[23] M. Benabdellah, M. Gharbi, N.Zahid, F. Regragui, E. H. Bouyakhf, Crypto-compression des images échographiques par la transformation de Faber-Schauder et l'algorithme DES,*Colloque International sur l'Informatique et ses Applications (IA'2006)*, ENSAO- Oujda, 31 octobre, 1 et 2 Novembre 2006.

[24] M. Benabdellah, M. Gharbi, N.Zahid, F. Regragui, E. H. Bouyakhf, Crypto-compression des images médicales par la transformation Multiéchelle de Faber-Schauder et l'algorithme AES, *2ème journées d'études Algéro-Francaises en imagerie médicale (JETIM'06)*, USTHB (Alger) et Corne d'or (Tipaza), Algérie, 21-22 Novembre 2006.

[25] M. Benabdellah, N. Zahid, F. Regragui, E. H. Bouyakhf, "Encryption-Compression of Echographic images using FMT transform and DES algorithm", *International INFOCOMP Journal of Computer Science*, March 2007, will be published in the following number.

Received: May 1, 2007